
COMPARATIVE EVALUATION OF LEARNING MODELS FOR BIONIC ROBOTS: NON-LINEAR TRANSFER FUNCTION IDENTIFICATIONS

• **Po-Yu Hsieh***

Graduate Institute of Architecture
National Yang Ming Chiao Tung University
Hsinchu, Taiwan
kevinhsieh870118@arch.nycu.edu.tw

• **June-Hao Hou**

Graduate Institute of Architecture
National Yang Ming Chiao Tung University
Hsinchu, Taiwan
jhou@arch.nycu.edu.tw

ABSTRACT

The control and modeling of bionic robot dynamics have increasingly adopted model-free control strategies using machine learning methods. Given the non-linear elastic nature of bionic robotic systems, learning-based methods provide reliable alternatives by utilizing numerical data to establish a direct mapping from actuation inputs to robot trajectories without complex kinematics models. However, for developers, the method of identifying an appropriate learning model for their specific bionic robots and further constructing the transfer function has not been thoroughly discussed. Thus, this research trains four types of models, including ensemble learning models, regularization-based models, kernel-based models, and neural network models, suitable for multi-input multi-output (MIMO) data and non-linear transfer function identification, in order to evaluate their (1) accuracy, (2) computation complexity, and (3) performance of capturing biological movements. This research encompasses data collection methods for control inputs and action outputs, selection of machine learning models, comparative analysis of training results, and transfer function identifications. The main objective is to provide a comprehensive evaluation strategy and framework for the application of model-free control.

Keywords Model-free Control · Bionic Continuum Robot · Learning-based method · Multi-input Multi-output · Transfer Function Identification

1 Introduction

One of the main objectives of robotics is to develop universal robots capable of learning and adapting to varying environments [Relaño et al., 2022]. While exhibiting exceptional dexterity and precision of performing tasks in predetermined conditions, traditional rigid robots often lack the flexibility and adaptability inherently [Trivedi et al., 2008].

Therefore, roboticists have drawn inspirations from nature, attempting to replicate the versatility and adaptive movements of biological systems. Biological entities maintain balance dynamically, constantly making micro-adjustments. This results in a stable yet agile locomotion that can quickly respond to disturbances. The inherent compliance and deformable body structure of biological systems often rely on the replacement of rigid joints. Instead, flexible joints with complex tension-compression synergy, which demonstrate high degrees of freedom, are commonly observed [Zappetti et al., 2020]. This unique feature ensures versatile movements with natural grace, fluidity, and sophistication, which conventional robots with fixed joints can hardly achieve.

In recent decades, new designs and approaches in bionic robotics have continuously emerged, with a specific focus on effectively modeling and controlling biological dynamics. Despite there are various types and applications of bionic robots, the control strategies are mainly based on either a model-based or model-free method. The model-based method involves detailed mathematical descriptions and kinematic calculations to build an analytical model. Its performance

*The scripts used in this study can be found on GitHub at the following repository: <https://github.com/poyuhs/model-free-robotics.git>

largely depends on the modeling accuracy and integrity. However, due to the elastic nature and deformable feature of bionic robots, this method is computationally intensive and robot specific [Vikas et al., 2015]. The dilemma of accuracy and computation complexity has led to a paradigm shift to the model-free method [Yu et al., 2024], which can be summarized as the following:

1. Data-driven: It relies heavily on collecting and utilizing data to identify the relationship between inputs (control parameters) and outputs (robot actions), which allows the robotic system to learn from experience and adapt to new situations.
2. End-to-End mapping: This method maps the actuation inputs directly to the robotic actions without requiring complex kinematics models, presenting less computational complexity.
3. Learning-based models: Various machine learning models are used to approximate the optimal control based on numerical data.

A comparative analysis conducted by Giorelli et al. [2015] has demonstrated that given the same inverse kinematics problem of a bionic tendon-driven robot, the model-free solution (feedforward neural network in this case) provides more accuracy and efficiency compared to the model-based analytical method (Jacobian method). In fact, ever since the early research on learning-based method for bionic robots, proposed by Vikas et al. [2015], were introduced, the applications have been explored in various fields, such as surgical manipulators using regression models [Xu et al., 2017], and bionic continuum robot using adaptive neural network [Melingui et al., 2015]. Recent studies have focused on using varying machine learning approaches to acquire an optimized transfer function due to its effectiveness of handling extensive numerical input-output data.

However, since the model-free method for the control of bionic robots is a relatively new field, the method of identifying an appropriate learning model for each specific robot and constructing transfer functions have not been thoroughly discussed. Therefore, this research aims to present a comparative evaluation of learning models based on accuracy, computational complexity, and the performance of replicating biological movements.

2 Background and Related Works

2.1 Description of the bionic robot

This research is based on a tendon-driven continuum robot with the tensegrity-based compliant mechanism (Figure 1) developed by Hsieh and Hou [2024]. Since much developments of robot structure and actuation system have been explored, this prototype provides a robust foundation for the research project. This bionic robot is inspired by the unique musculoskeletal features of vertebrates, which utilize the tension-compression synergy to perform adaptability. The unit of this robot structure is composed of three tendon actuators, hexagonal plates, struts, and rhombic cables, which respectively represent the tendons, vertebrae, bones, and muscles in physiology of vertebrates. Furthermore, these elements are parametrized, which allows developers to decide the number of segments (N) and each individual dimension.

The actuator of this robot relies on a tendon-driven technique, grafting the parallel compliant mechanism onto a tensegrity-based robot body. This actuation mechanism effectively leverages the self-balancing behavior of tensegrity structures. Once pulling forces are applied, the robot body will gradually change its configuration to achieve the new equilibrium, which shares a similarity with biological movements. By manipulating the length variations of each tendon (ΔL), the robot is able to perform a wide range of motions with inherent high compliance.

Nevertheless, the modeling and control of its dynamics still require further identifications. The control method proposed in this previous paper relies on an inverse kinematics model similar to delta robots, which lacks the consideration of the non-linear elastic nature of continuum robots.

2.2 Decoupled transfer function

To achieve a better control of the robot, we utilize the transfer function proposed by Relaño et al. [2022]. This transfer function focuses on tendon-driven continuum robots with three tendon actuators, which is applicable in this context. It is demonstrated by a decoupling mathematical process, aiming to identify the equations of control inputs and action outputs. The variables in this transfer function are yaw and pitch angles (α, β) and variations of the tendon lengths (L_1, L_2, L_3), assuming two degrees of freedom (DOF) for simplifications. Additionally, it is also assumed that $L_1 + L_2 + L_3 = 0$, indicating the entire continuum robot remains the same angle of curvature while bending. Given these assumptions, the transfer function can be described as:

$$L_1 = \frac{\alpha}{1.5} \quad (1)$$

$$L_2 = \frac{\beta}{1.732} - \frac{\alpha}{3} \quad (2)$$

$$L_3 = -\frac{\beta}{1.732} - \frac{\alpha}{3} \quad (3)$$

To validate the actual performance, we have applied these control algorithms to the robot simulation. The validation experiment is conducted by inserting a series of target yaw and pitch angles from -90° to 90° at an interval of 10, and collecting the length variation values of each tendon actuator. The evaluation of yaw and pitch movements are divided into two separate processes, which means that the simulation inputs α and β are non-zero and zero value alternatively. This allows the vertical and horizontal movements to be clearly viewed separately. Four conditions with different number of segments ($N=1, 2, 3, 4$) are selected as the subjects to test out the impact of value N on the actual movements. Figure 2, 3, 4, and 5 illustrate the robot's actual motions over time (t), with (a) the physical configuration with $t=0$, (b) the variation of yaw angle (α), and (c) the pitch angle (β). The performance analysis reveals several key observations:

- **Impact of segment number:** Increasing the number of segments (N) generally improves the robot's ability to achieve the desired motions. This is attributed to the increased degrees of freedom provided by additional segments, allowing for more precise control of the yaw and pitch angles. Configurations with $N=1$ to $N=3$ inherently exhibit limited motion ranges due to the restricted degrees of freedom. These configurations struggle to meet the desired yaw and pitch angles accurately.
- **Trade-offs with increased segments:** While adding more segments enhances performance, it also introduces greater structural complexity. The influence of gravitational loads become more pronounced as well, potentially leading to stability issues and an increased computational load.
- **Optimal performance with $N=4$:** The configuration with four segments demonstrates the best performance, closely approximating the desired motions. This configuration strikes a balance between flexibility and structural complexity, making it the most efficient setup for the following research.

However, even with the optimal configuration ($N=4$), there are still observable deviations between the actual and desired motions (Figure 6). These discrepancies indicate that the original transfer functions are not fully adequate for capturing the non-linear dynamics of the bionic tendon-driven robot. To address this issue, the following sections explore the use of machine learning models to derive more accurate and robust transfer functions. By leveraging data-driven approaches, we aim to improve the control and modeling of the robot's dynamics, thereby enhancing its overall performance.

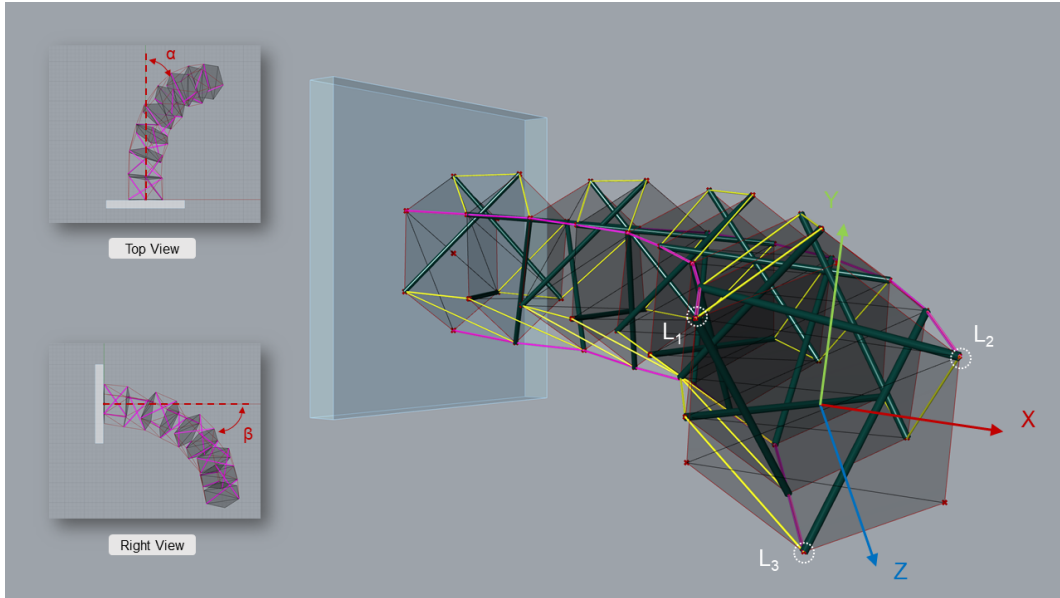
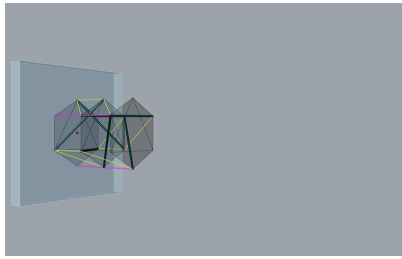
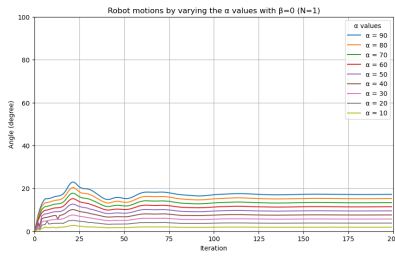


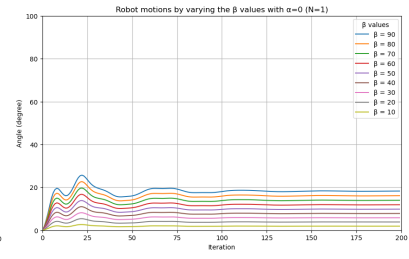
Figure 1: View of the tendon-driven continuum robot.



(a) N=1

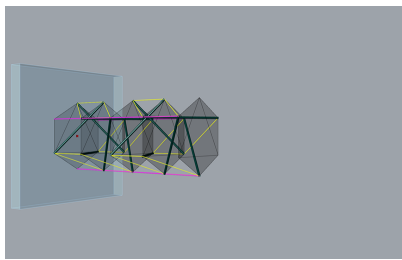


(b) α over time

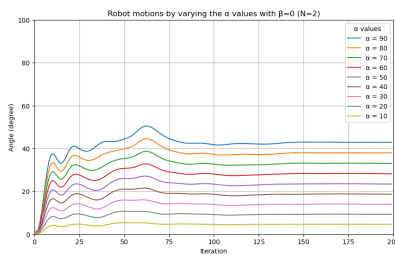


(c) β over time

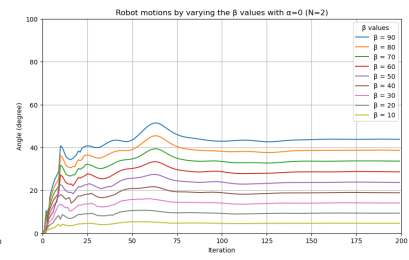
Figure 2: Actual motions with N=1.



(a) N=2

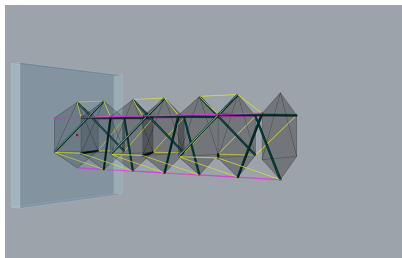


(b) α over time

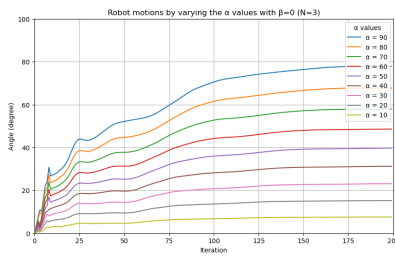


(c) β over time

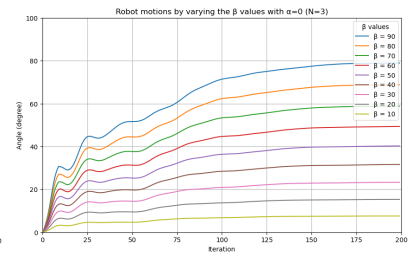
Figure 3: Actual motions with N=2.



(a) N=3.

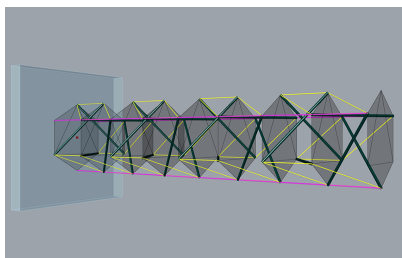


(b) α over time

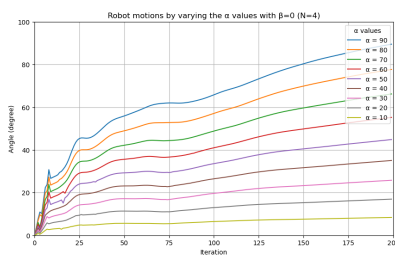


(c) β over time

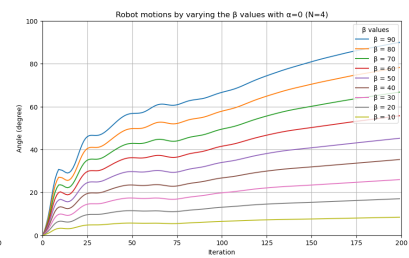
Figure 4: Actual motions with N=3.



(a) N = 4



(b) α over time



(c) β over time

Figure 5: Actual motions with N=4.

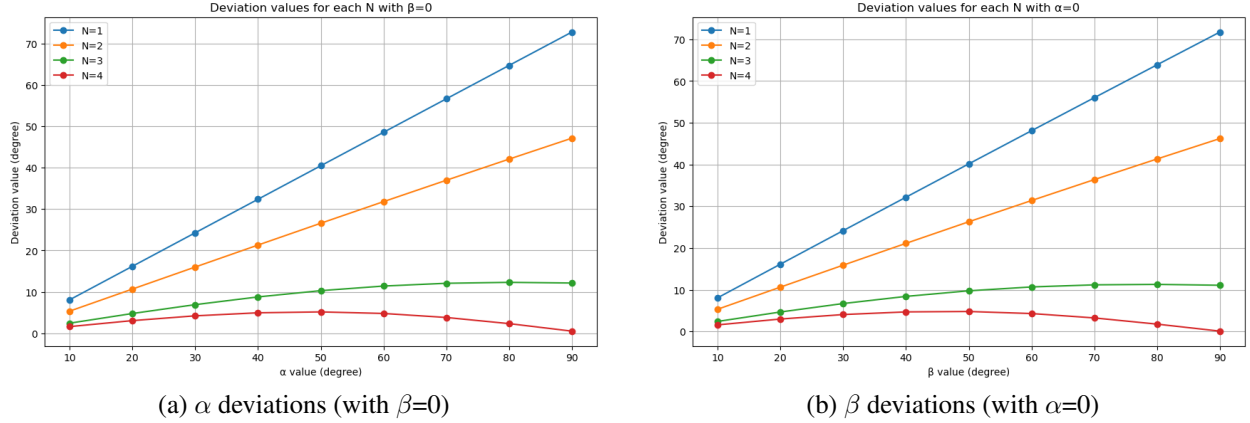


Figure 6: Deviations for each N.

3 Methods

The proposed research methodology is comprised of four principal phases (Figure 7). In the preliminary phase, data collection is conducted using physics simulations to capture robotic motions (yaw and pitch angles) and corresponding actuation parameters (length variations of each tendon). Subsequently, eight different learning models suitable for non-linear data are selected and trained with the dataset. A comparative analysis is then conducted to evaluate the performance of each model, including accuracy and computation costs. Eventually, the transfer functions derived from each learning model are sent back to the robot simulation to validate the actual locomotion based on biomimetic metrics.

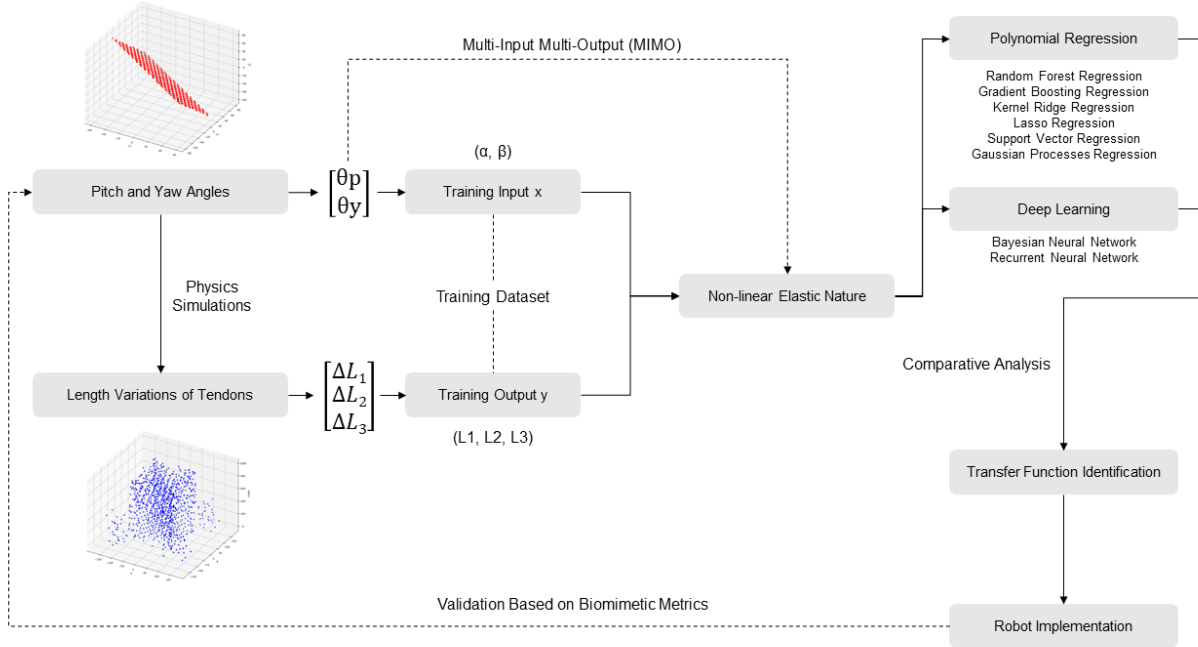


Figure 7: Methodology.

3.1 Data collection

The training dataset for this research was constructed to capture the complex dynamics (in full range of possible motions) of a bionic tendon-driven robot in a multi-input multi-output (MIMO) condition. The data collection process involved simulating various pitch (α) and yaw (β) angles (Figure 8) and recording the corresponding variations (Figure 8) in tendon lengths (L_1, L_2, L_3).

To ensure the robustness and generalizability of the training dataset, the input angles were varied systematically, and multiple measurements were taken for each angle combination. This approach ensures that the machine learning models trained on this dataset can generalize well to unseen data, thereby enhancing their predictive performance and reliability.

This data collection process was conducted using a physics-based simulation environment (Grasshopper within Rhino). This platform allows for precise control and measurement of the robot's movements, enabling the collection of high-fidelity data.

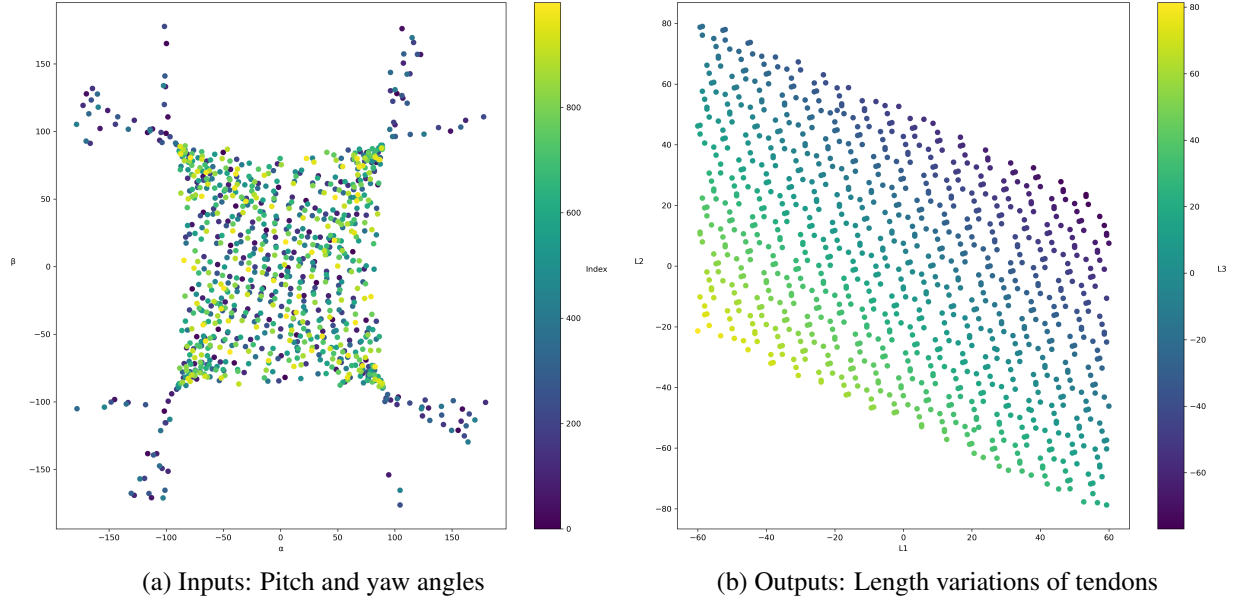


Figure 8: Training data collection.

3.2 Learning model selection

In this section, we evaluate the performance of eight different machine learning models to derive transfer functions for bionic tendon-driven robots. The selected models are categorized into four sets: ensemble learning models, regularization-based models, kernel-based models, and neural network models. These models were selected based on their suitability for handling non-linear, MIMO data, which can be summarized as the following:

Ensemble Learning Models

3.2.1 Random Forest (RF)

Reason for selection: Random Forest is an ensemble learning method that builds multiple decision trees and merges their outcomes to improve accuracy and prevent overfitting. It is robust to noise and can capture non-linear relationships.

Mathematical basis: Random Forest aggregates the predictions of numerous decision trees, which are constructed by randomly sampling the data and features. This reduces variance and enhances generalization.

3.2.2 Gradient Boosting (GB)

Reason for selection: Gradient Boosting builds an ensemble of weak prediction models, typically decision trees, and optimizes them iteratively to minimize the loss function. It is effective for capturing intricate patterns in data and handling non-linear dependencies.

Mathematical basis: Gradient Boosting sequentially adds trees to the model, where each new tree corrects the errors made by the previous ones. This process is guided by gradient descent on the loss function.

Regularization-Based Models

3.2.3 Lasso Regression

Reason for selection: Lasso Regression (Least Absolute Shrinkage and Selection Operator) is a linear model that performs both variable selection and regularization, enhancing prediction accuracy and interpretability. It is useful for high-dimensional datasets where some features may be irrelevant.

Mathematical basis: Lasso minimizes the residual sum of squares with an l_1 penalty term, which encourages sparsity in the model coefficients.

3.2.4 Ridge Regression

Reason for selection: Ridge Regression addresses multicollinearity issues by adding an l_2 penalty to the loss function. It shrinks the model coefficients, making it more robust to overfitting and capable of handling correlated features.

Mathematical basis: Ridge minimizes the residual sum of squares with an l_2 penalty term, which reduces the model complexity by shrinking the coefficients.

Kernel-Based Models

3.2.5 Support Vector Regressor (SVR)

Reason for selection: SVR extends support vector machines to regression problems. It is effective for high-dimensional spaces and can model non-linear relationships through kernel functions.

Mathematical basis: SVR finds a hyperplane in a high-dimensional space that best fits the data while minimizing a margin of tolerance. Kernel functions transform the input space to a higher-dimensional space where linear separation is possible.

3.2.6 Gaussian Process Regressor (GPR)

Reason for selection: GPR provides a probabilistic approach to regression, offering not only predictions but also uncertainty estimates. It is highly flexible and can model complex non-linear relationships.

Mathematical basis: GPR assumes a Gaussian prior over functions and updates the posterior based on observed data. The predictions are made using a kernel function that measures the similarity between points.

Neural Network Models

3.2.7 Bayesian Neural Network (BNN)

Reason for selection: BNN incorporates Bayesian inference into neural networks, providing probabilistic predictions and uncertainty estimates. It is robust to overfitting and can model non-linear relationships effectively.

Mathematical basis: BNNs place a prior distribution over the network weights and update the posterior distribution based on observed data, offering a measure of uncertainty in predictions.

3.2.8 Recurrent Neural Network (RNN)

Reason for selection: RNNs are designed to handle sequential data and temporal dependencies, making them suitable for modeling dynamic systems. They can capture the time-dependent behavior of tendon-driven robots.

Mathematical basis: RNNs have cyclic connections, allowing information to persist across time steps. This makes them capable of learning from sequences of data.

4 Results

4.1 Performance evaluation

The training process (Figure 9 to 16) for each learning model is evaluated by comparing the predicted values (red) against the actual values (blue) for L1, L2, and L3, along with the absolute error (gray).

For RF (Figure 9) and GPR models (Figure 14), the predictions for L1, L2, and L3 exhibit high variability with significant deviations between the predicted and actual values, indicating considerable errors across all samples. The predictions from GB model (Figure 10) are closely aligned with the actual values, indicating superior accuracy and stability. It demonstrates the best performance among the models. For regularization-based models, the predictions from Lasso (Figure 11) and Ridge (Figure 12) regression models both show variability and deviations. The absolute error indicates moderate performance, with some significant errors. For SVR model (Figure 13), the predictions show moderate alignment with the actual values, suggesting a balanced performance. The predictions from BNN (Figure 15) and RNN (Figure 16) are closely aligned with the actual values, demonstrating a more stable performance and high accuracy.

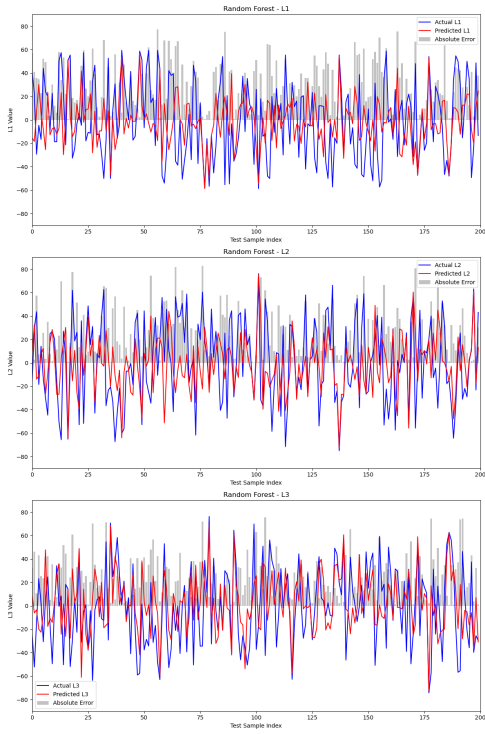


Figure 9: Random Forest.

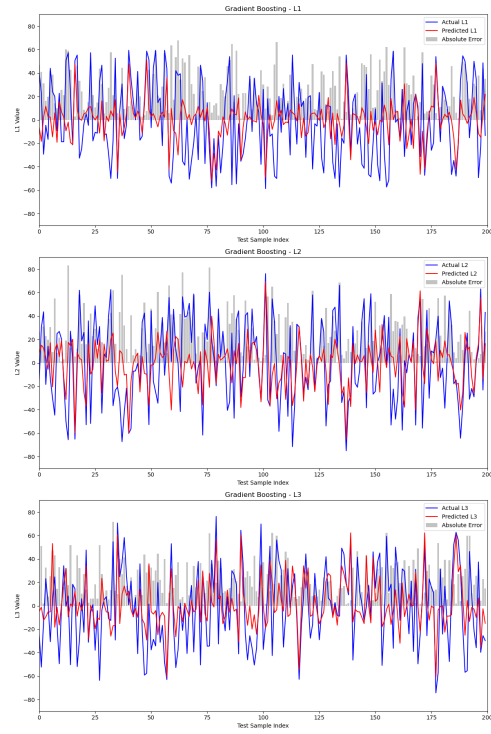


Figure 10: Gradient Boosting.

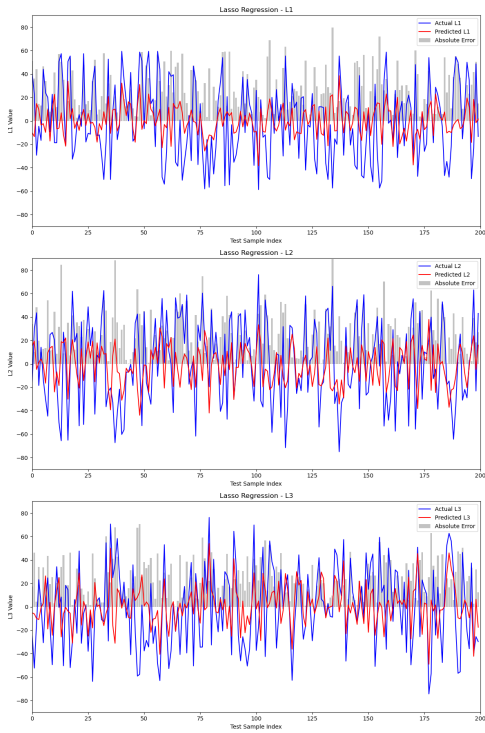


Figure 11: Lasso Regression.

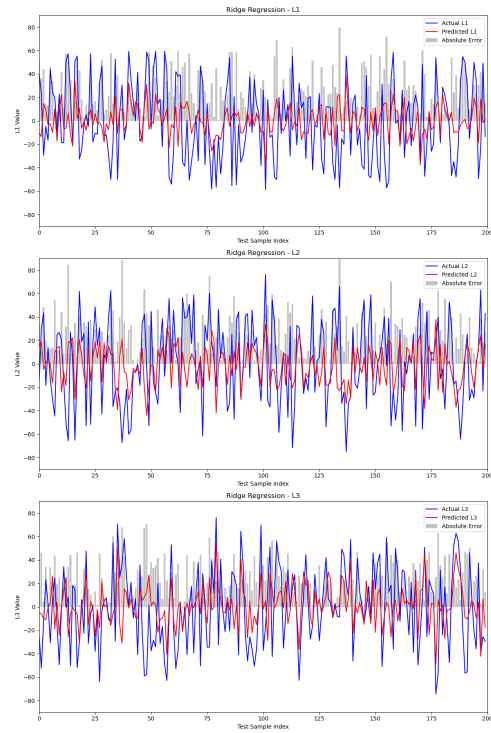


Figure 12: Ridge Regression.

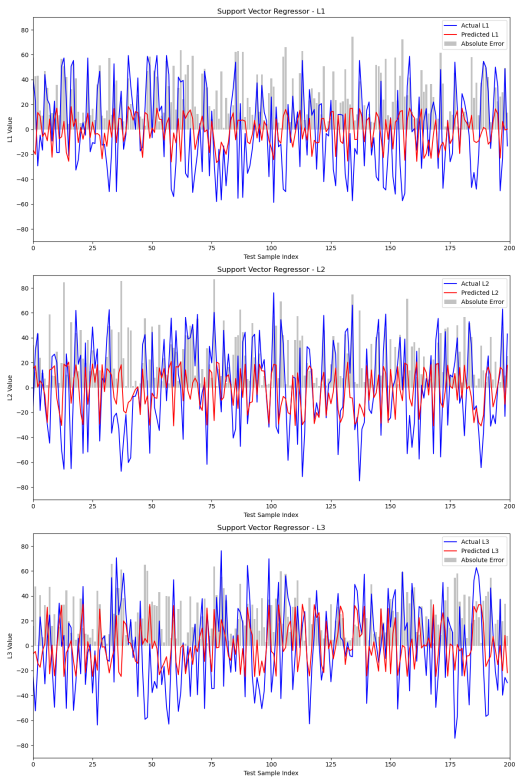


Figure 13: Support Vector Machine.

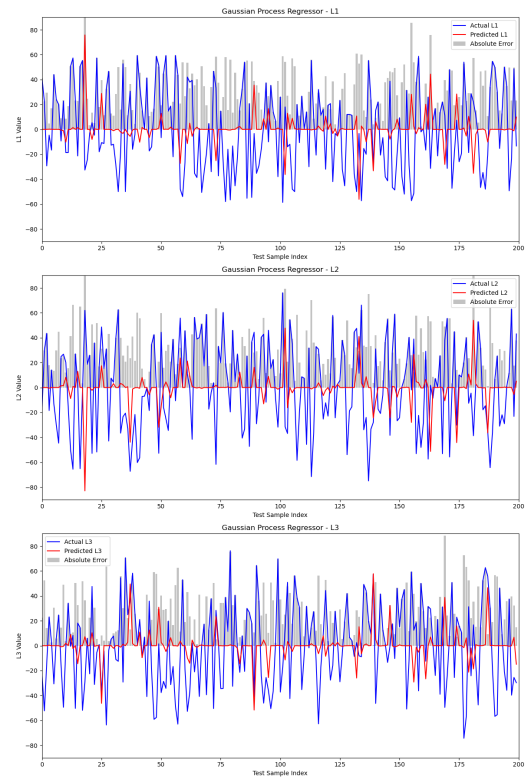


Figure 14: Gaussian Process Regression.

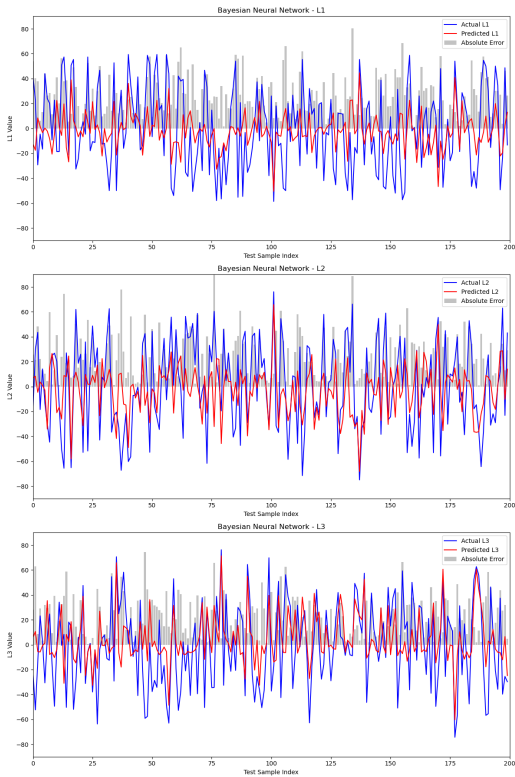


Figure 15: Bayesian Neural Network.

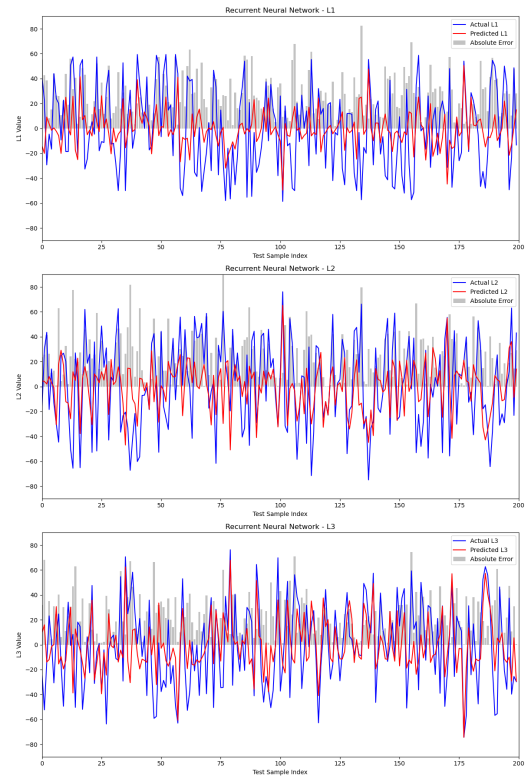


Figure 16: Recurrent Neural Network.

Table 1: Performance metrics of different learning models

| Model | MSE | MAE | Computation Time (s) |
|---------------------------|--------------|------------------|----------------------|
| Random Forest | 1058.216 120 | 25.694 405 | 1.760 020 |
| Gradient Boosting | 866.197 726 | 23.549753 | 0.526 898 |
| Ridge | 927.343 365 | 24.714 297 | 0.013705 |
| Lasso | 927.339 126 | 24.714 440 | 0.013146 |
| Support Vector | 935.759 171 | 24.398921 | 0.243 148 |
| Gaussian Processes | 1243.854 615 | 29.352 238 | 1.734 590 |
| BNN | 882.995 994 | 24.169767 | 28.626 474 |
| RNN | 876.559 293 | 23.967265 | 32.470 035 |

Table 1 presents an overall performance of each learning model, including mean square error (MSE), mean absolute error (MAE), and computation time. While GB and SVR exhibit significant scores in MAE, their counterparts RF and GPR show worse performance, indicating the instability of ensemble learning and kernel-based models for bionic robots. Neural network models BNN and RNN, on the other hand, demonstrate a more stable solution with high accuracy. However, it requires more computational complexity. Regarding regularization-based models, despite their lower accuracy, Ridge and Lasso models exhibit significantly reduced computation time, making them efficient for real-time applications. This efficiency is crucial for bionic robots, where adaptability and responsiveness are more important than extreme precision, aligning with the goals of replicating biological movements.

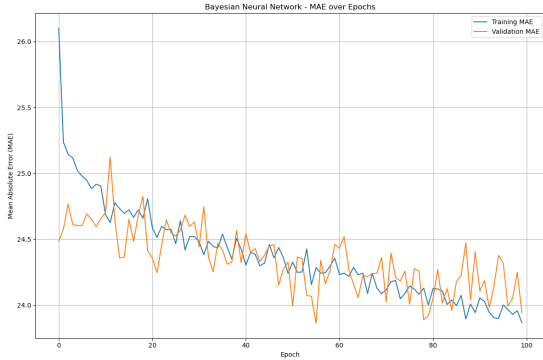


Figure 17: BNN: MAE over epochs.

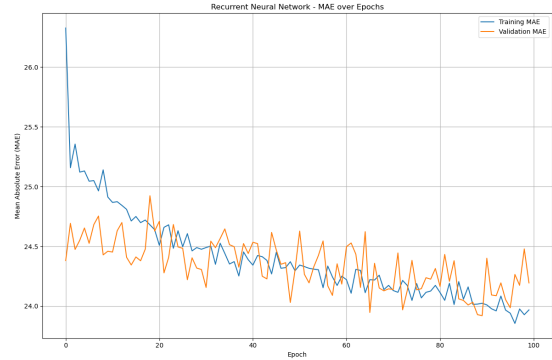


Figure 18: RNN: MAE over epochs.

The research further explore the generalization capabilities of the neural network models for robotic learning by presenting the training and validation MAE over 100 epochs (Figure 17 and 18). Both training MAE of BNN and RNN exhibit a sharp decline during the initial 20 epochs, indicating that these models can quickly learn from the training data. The BNN model displays a stable validation MAE curve, while the RNN model shows slight fluctuations, reflecting its sensitivity to temporal variations in the data. Overall, both models are capable of capturing the complex dynamics of bionic tendon-driven robots, making them suitable for developing accurate, robust model-free control strategies.

4.2 Transfer function identification

To capture non-linear relationships between the input variables (α, β) and the output variables (L_1, L_2, L_3) , polynomial features are generated. For a second-degree polynomial, the feature set includes:

$$\{1, \alpha, \beta, \alpha^2, \alpha\beta, \beta^2\}$$

Mathematically, the polynomial features $\Phi(\mathbf{x})$ for input vector $\mathbf{x} = [\alpha, \beta]^T$ can be expressed as:

$$\Phi(\mathbf{x}) = [1, \alpha, \beta, \alpha^2, \alpha\beta, \beta^2]^T$$

Given the polynomial features, we fit a linear regression model to represent the non-linear relationship between the inputs and outputs. The regression model for each output L_i (where $i \in \{1, 2, 3\}$) can be formulated as:

$$L_i = w_{i0} + w_{i1}\alpha + w_{i2}\beta + w_{i3}\alpha^2 + w_{i4}\alpha\beta + w_{i5}\beta^2$$

where w_{ij} are the coefficients of the polynomial regression model for the i -th output and j -th term.

The coefficients obtained from the polynomial regression model are used to construct the transfer function equations. For each output L_i , the transfer function T_i can be expressed as:

$$T_i(\alpha, \beta) = w_{i0} + w_{i1}\alpha + w_{i2}\beta + w_{i3}\alpha^2 + w_{i4}\alpha\beta + w_{i5}\beta^2$$

The process of identifying transfer functions using polynomial regression is applied to the predictions made by each machine learning model. This involves the following steps:

1. **Training the machine learning model:** Each machine learning model is trained to predict the outputs $\hat{L}_1, \hat{L}_2, \hat{L}_3$ from the inputs α, β .
2. **Generating polynomial features:** Polynomial features are generated from the inputs α, β .
3. **Fitting polynomial regression:** A polynomial regression model is fitted using the polynomial features and the predicted outputs from the machine learning model.
4. **Constructing transfer functions:** The coefficients and intercepts from the polynomial regression model are used to construct the transfer function equations.

Thus, the transfer functions of each regression model can be derived as:

Random Forest

$$L1 = 1.0197 + (0.1833)\alpha + (-0.0700)\beta + (-0.0001)\alpha^2 + (0.0002)\alpha\beta + (-0.0001)\beta^2 \quad (4)$$

$$L2 = -0.4349 + (-0.0089)\alpha + (0.2548)\beta + (0.0002)\alpha^2 + (-0.0004)\alpha\beta + (-0.0003)\beta^2 \quad (5)$$

$$L3 = -0.5848 + (-0.1744)\alpha + (-0.1848)\beta + (-0.0001)\alpha^2 + (0.0003)\alpha\beta + (0.0004)\beta^2 \quad (6)$$

Gradient Boosting

$$L1 = 1.0197 + (0.1833)\alpha + (-0.0700)\beta + (-0.0001)\alpha^2 + (0.0002)\alpha\beta + (-0.0001)\beta^2 \quad (7)$$

$$L2 = -0.4349 + (-0.0089)\alpha + (0.2548)\beta + (0.0002)\alpha^2 + (-0.0004)\alpha\beta + (-0.0003)\beta^2 \quad (8)$$

$$L3 = -0.5848 + (-0.1744)\alpha + (-0.1848)\beta + (-0.0001)\alpha^2 + (0.0003)\alpha\beta + (0.0004)\beta^2 \quad (9)$$

Ridge Regression

$$L1 = 0.1783 + (0.1839)\alpha + (-0.0704)\beta \quad (10)$$

$$L2 = -0.7694 + (-0.0106)\alpha + (0.2540)\beta \quad (11)$$

$$L3 = 0.5911 + (-0.1733)\alpha + (-0.1835)\beta \quad (12)$$

Lasso Regression

$$L1 = 0.1782 + (0.1839)\alpha + (-0.0704)\beta \quad (13)$$

$$L2 = -0.7693 + (-0.0106)\alpha + (0.2540)\beta \quad (14)$$

$$L3 = 0.5911 + (-0.1733)\alpha + (-0.1835)\beta \quad (15)$$

Support Vector Regressor

$$L1 = 1.0197 + (0.1833)\alpha + (-0.0700)\beta + (-0.0001)\alpha^2 + (0.0002)\alpha\beta + (-0.0001)\beta^2 \quad (16)$$

$$L2 = -0.4349 + (-0.0089)\alpha + (0.2548)\beta + (0.0002)\alpha^2 + (-0.0004)\alpha\beta + (-0.0003)\beta^2 \quad (17)$$

$$L3 = -0.5848 + (-0.1744)\alpha + (-0.1848)\beta + (-0.0001)\alpha^2 + (0.0003)\alpha\beta + (0.0004)\beta^2 \quad (18)$$

Gaussian Process Regressor

$$L1 = 1.0197 + (0.1833)\alpha + (-0.0700)\beta + (-0.0001)\alpha^2 + (0.0002)\alpha\beta + (-0.0001)\beta^2 \quad (19)$$

$$L2 = -0.4349 + (-0.0089)\alpha + (0.2548)\beta + (0.0002)\alpha^2 + (-0.0004)\alpha\beta + (-0.0003)\beta^2 \quad (20)$$

$$L3 = -0.5848 + (-0.1744)\alpha + (-0.1848)\beta + (-0.0001)\alpha^2 + (0.0003)\alpha\beta + (0.0004)\beta^2 \quad (21)$$

Additionally, a comparative graph (Figure 19 and 20) is presented to identify the difference between the optimal transfer functions (derived from GB model) and the original ones. The changing in geometry can be considered as a fine-tuning result after the training process.

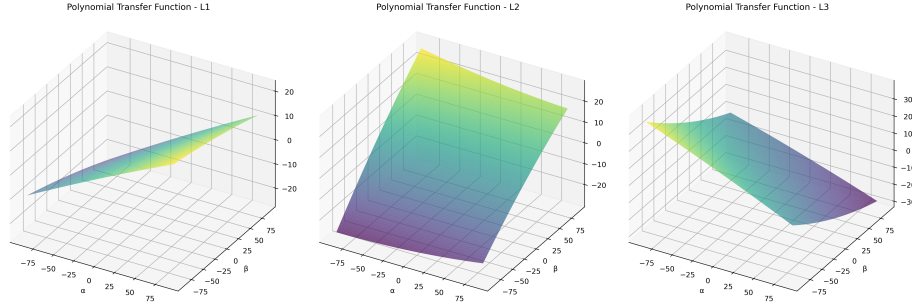


Figure 19: Optimal transfer functions.

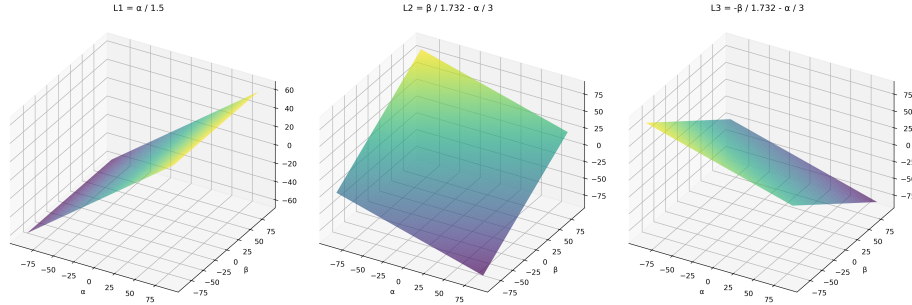


Figure 20: Original transfer functions.

As for neural network models, BNN and RNN do not provide direct transfer functions due to their implicit nature (multiple layers of interconnected neurons and non-linear activation functions). Yet, they are still capable of predicting accurate control parameters.

5 Conclusions

This research focuses on the model-free methods for bionic tendon-driven robots using learning models to optimize the modeling and control of their complex dynamics. Due to the lack of comprehensive evaluations of various machine learning methods for bionic robots, roboticists often encounter difficulties in identifying an effective learning model and developing optimized transfer functions. To address these challenges, we employ eight different models suitable for MIMO, non-linear data. The training dataset is constructed by simulating various yaw and pitch angles (α , β) in a physics-based environment and recording the corresponding tendon length variations (L_1 , L_2 , L_3). Each model has been trained and evaluated based on three key performance metrics: accuracy (measured by MSE and MAE), computation time, and biomechanical relevance. Ensemble learning and kernel-based models display significant score in MAE but struggling with stability. Neural network models also show promising results with high accuracy, stability, high learning efficiency, despite they are computationally intensive. Regularization-based models require less computational cost, making them efficient alternatives for real-time applications.

References

- Carlos Relaño, Jorge Muñoz, Concepción A Monje, Santiago Martínez, and Daniel González. Modeling and control of a soft robotic arm based on a fractional order control approach. *Fractal and Fractional*, 7(1):8, 2022. URL <https://doi.org/10.3390/fractalfract7010008>.
- Deepak Trivedi, Christopher D Rahn, William M Kier, and Ian D Walker. Soft robotics: Biological inspiration, state of the art, and future research. *Applied bionics and biomechanics*, 5(3):99–117, 2008. URL <https://doi.org/10.1080/11762320802557865>.
- Davide Zappetti, Roc Arandes, Enrico Ajanic, and Dario Floreano. Variable-stiffness tensegrity spine. *Smart Materials and Structures*, 29(7):075013, 2020. URL <https://doi.org/10.1088/1361-665X/ab87e0>.
- Vishesh Vikas, Piyush Grover, and Barry Trimmer. Model-free control framework for multi-limb soft robots. In *2015 IEEE/RSJ International Conference on Intelligent Robots and Systems (IROS)*, pages 1111–1116. IEEE, 2015. URL <https://doi.org/10.1109/IR0S.2015.7353509>.
- Zhilin Yu, Alin Duan, Zhisen Zhu, and Wenling Zhang. Biomimetic soft-legged robotic locomotion, interactions and transitions in terrestrial, aquatic and multiple environments. *Sustainable Materials and Technologies*, page e00930, 2024. URL <https://doi.org/10.1016/j.susmat.2024.e00930>.
- Michele Giorelli, Federico Renda, Marcello Calisti, Andrea Arienti, Gabriele Ferri, and Cecilia Laschi. Neural network and jacobian method for solving the inverse statics of a cable-driven soft arm with nonconstant curvature. *IEEE Transactions on Robotics*, 31(4):823–834, 2015. URL <https://doi.org/10.1109/TR0.2015.2428511>.
- Wenjun Xu, Jie Chen, Henry Y.K. Lau, and Hongliang Ren. Data-driven methods towards learning the highly nonlinear inverse kinematics of tendon-driven surgical manipulators. *The International Journal of Medical Robotics and Computer Assisted Surgery*, 13(3):e1774, 2017. URL <https://onlinelibrary.wiley.com/doi/abs/10.1002/rcs.1774>.
- Achille Melingui, Othman Lakhal, Boubaker Daachi, Jean Bosco Mbede, and Rochdi Merzouki. Adaptive neural network control of a compact bionic handling arm. *IEEE/ASME Transactions on Mechatronics*, 20(6):2862–2875, 2015. URL <https://doi.org/10.1109/TMECH.2015.2396114>.
- Po-Yu Hsieh and June-Hao Hou. A biomimetic robotic system with tensegrity-based compliant mechanism. In *Proceedings of the 29th CAADRIA Conference, Singapore*, volume 3, pages 131–140, 2024. URL https://papers.cumincad.org/cgi-bin/works/Show?caadria2024_76.